

See discussions, stats, and author profiles for this publication at: <https://www.researchgate.net/publication/231674072>

# Infrared Ellipsometry of Langmuir–Blodgett Films on Gold. Toward Interpreting the Molecular Orientation

ARTICLE *in* LANGMUIR · JULY 2002

Impact Factor: 4.46 · DOI: 10.1021/la0201117

---

CITATIONS

26

---

READS

22

5 AUTHORS, INCLUDING:



D. Tsankov

Bulgarian Academy of Sciences

41 PUBLICATIONS 420 CITATIONS

SEE PROFILE

# Infrared Ellipsometry of Langmuir–Blodgett Films on Gold. Toward Interpreting the Molecular Orientation

D. Tsankov,<sup>†,‡</sup> K. Hinrichs,<sup>\*,†</sup> E. H. Korte,<sup>†</sup> R. Dietel,<sup>§</sup> and A. Röseler<sup>†</sup>

*Institute of Spectrochemistry and Applied Spectroscopy—Department Berlin, Albert-Einstein-Strasse 9, 12489 Berlin, Germany, and Institute of Thin Film Technology and Microsensorics, Kantstrasse 55, 14513 Teltow, Germany*

*Received February 1, 2002. In Final Form: May 6, 2002*

Langmuir–Blodgett (LB) films (nine double layers) of 2-[4-(*N*-dodecanoylamino)phenyl]-5-(4-nitrophenyl)-1,3,4-oxadiazole on gold were analyzed by means of infrared (IR) ellipsometry followed by theoretical interpretation of the measured spectra in a uniaxial anisotropic layer model. The same material in a KBr pellet was investigated by IR transmission spectroscopy. The evaluation provided data for vibrational band parameters, necessary for elucidation of the molecular orientation. The LB film was then annealed at 130 °C since structural changes due to the thermal treatment were expected to occur, and hence the films before and after annealing can serve as model systems with different molecular orientations. The data revealed that the molecules were hydrogen bonded both in a pellet and as LB films. These bonds were only partly disrupted due to the thermal treatment and play the role of an additional factor stabilizing the film structure. After annealing, a change of about 14° was calculated from ellipsometric spectra for the head NO<sub>2</sub> group orientation with respect to the surface plane, which would provoke a commensurable decrease of the aliphatic chain tilt angle. The presented results demonstrate the capabilities of infrared spectroscopic ellipsometry not only to determine the film optical constants and thickness, but also to probe some aspects of the molecular orientation.

## Introduction

Langmuir–Blodgett (LB) films have attracted substantial interest over the last two decades since they have potential for some practical applications in sensors, nonlinear optics, and electronic devices and keep serving as model systems for studying ordered films.<sup>1–3</sup> Extensive research including infrared (IR) spectroscopy, second-harmonic generation (SHG), atomic force microscopy (AFM), ellipsometry, and X-ray diffraction studies has been performed<sup>1,2</sup> aiming to elucidate the inherent molecular structure of the film and the relative orientation of the aliphatic chains with respect to the substrate surface. A large segment of the existing experimental data have been accumulated by IR studies. In attempts to better characterize the intrinsic molecular orientation, both transmission measurements on IR transparent substrates and reflection measurements on metallic, dielectric, or semiconductor surfaces have been carried out.<sup>4–7</sup> While normal incidence IR transmission spectra of LB films display bands due to vibrational transition moments projected into directions within the surface plane, reflection spectra on metallic substrates exhibit only bands due

to transition moments projected perpendicular to the surface according to a so-called “surface selection rule”.<sup>8</sup> The existing IR data reveal that the long-chain molecules constituting the LB films are highly ordered in every individual monolayer and the directions of their aliphatic chains are slightly deviated from the surface normal. Some SHG studies carried out on noncentrosymmetric Langmuir–Blodgett films such as 2-docosylamino-5-nitropyridine (DCANP)<sup>9,10</sup> and *n*-docosyl-2-methyl-4-nitroaniline (DCMNA)<sup>11</sup> claimed an unusual herringbone structure of the Y-type multilayers and considerable bilayer spacing. In this case the noncentrosymmetry has been attributed to a unique alignment of the chromophores in the substrate plane and in a second plane along the dipping direction.<sup>9–11</sup>

IR analysis often needs spectral simulations, invoked to confirm the spectral distribution of the infrared intensities and hence to resolve the spatial orientation of characteristic molecular groups. These calculations usually demand knowledge of the high-frequency optical constants and the thickness. Typically, these data are provided by ellipsometric experiments. UV–vis ellipsometry is the most frequently used method for this purpose and is able to supply accurate data for the film thickness. However, the high-frequency refractive index ( $n_\infty$ ) determined from UV spectra does not necessarily coincide with the one obtainable from infrared measurements. Conversely, infrared reflection absorption spectroscopy can be used to obtain the IR optical constants via Kramers–Kronig transformation, but lacks the film thickness. The method that is able to give both the accurate film optical

\* To whom correspondence should be addressed. E-mail: hinrichs@isas-berlin.de.

<sup>†</sup> Institute of Spectrochemistry and Applied Spectroscopy—Department Berlin.

<sup>‡</sup> Permanent address: Institute of Organic Chemistry, Bulgarian Academy of Sciences, BG-1113 Sofia, Bulgaria.

<sup>§</sup> Institute of Thin Film Technology and Microsensorics.

(1) Roberts, G. G. In *Langmuir–Blodgett Films*; Roberts, G., Ed.; Plenum Press: London, 1990; pp 317–411.

(2) Ulman, A. *An Introduction to Ultrathin Organic Films*; Academic Press: San Diego, 1991; Chapter 1.

(3) Petty, M. C. *Thin Solid Films* **1992**, 210/211, 417–426.

(4) Allara, D. L.; Swalen, J. D. *J. Phys. Chem.* **1982**, 86, 2700–2704.

(5) Rabolt, J. F.; Burns, F. C.; Schlotter, N. E.; Swalen, J. D. *J. Chem. Phys.* **1983**, 78, 946–952.

(6) Umemura, J.; Kamata, T.; Kawai, T.; Takenaka, T. *J. Phys. Chem.* **1990**, 94, 62–67.

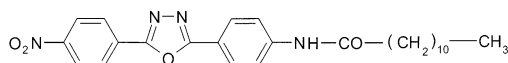
(7) Buffeteau, T.; Blaudez, D.; Pere, E.; Desbat, B. *J. Phys. Chem.* **1999**, 103, 5020–5027.

(8) Greenler, R. G. *J. Chem. Phys.* **1966**, 44, 310–335.

(9) Decher, G.; Tieke, B.; Bosshard, C.; Günter, J. *Chem. Soc., Chem. Commun.* **1988**, 933–934.

(10) Kajikawa, K.; Wang, L.-M.; Isoshima, T.; Wada, T.; Knoll, W.; Sasabe, H.; Okada, S.; Nakanishi, H. *Thin Solid Films* **1996**, 284–285, 612–614.

(11) Howarth, V.; Asai, N.; Kishii, N.; Fujiwara, I. *Appl. Phys. Lett.* **1992**, 61, 1616–1618.



2-[4-(N-Dodecanoylamino)phenyl]-5-(4-nitrophenyl)-1,3,4-oxadiazole

**Figure 1.** Chemical formula of the investigated compound.

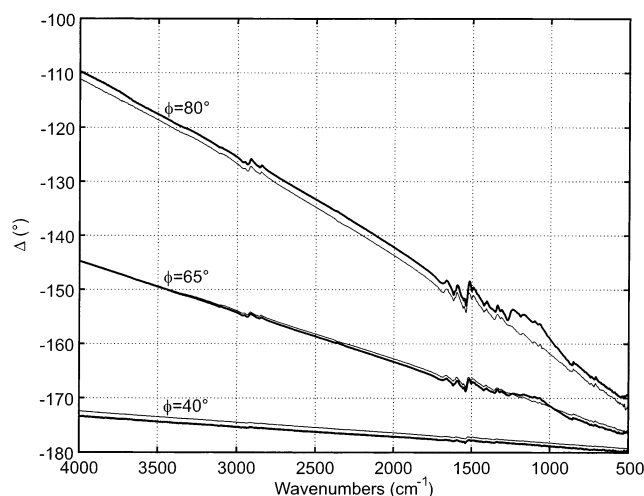
constants and thickness in one measurement is IR spectroscopic ellipsometry. Backed up by suitable model calculations, it is capable of probing aspects of the space orientation of molecules constituting the film. This has recently been demonstrated in the study of the molecular orientation of self-assembled monolayers.<sup>12</sup> So far the existing IR ellipsometric studies of LB films have been constrained mainly to evaluating film optical constants (refractive index  $n$  and absorption index  $k$ ) and thickness ( $d$ ).<sup>13,14</sup> In this paper we aim to demonstrate the potential of IR ellipsometry as a versatile technique for analyzing both the optical and structural properties of such films.

An LB film consisting of nine double layers of 2-[4-(N-dodecanoylamino)phenyl]-5-(4-nitrophenyl)-1,3,4-oxadiazole (Figure 1) was prepared and studied by IR ellipsometry. Some previous X-ray specular reflectivity results<sup>15</sup> suggested Y-type multilayer formation and uniaxial symmetry of the LB film. The ellipsometric spectra were simulated by best-fit calculations to determine vibrational band parameters and subsequently to deduce the molecular orientation. The LB films were annealed for 10 min at 130 °C to identify the changes in the molecular orientation already detected by X-ray experiments.<sup>15</sup>

A preliminary report addressing some elements of progress in this project has been published recently.<sup>16</sup> Here we present the complete analysis of the ellipsometric spectra, propose band assignments, and discuss the orientation of the film molecules.

## Experimental Section

**(A) Ellipsometry of Thin Films.** Linearly polarized light becomes in general elliptically polarized upon reflection at a plane surface. The polarization state of the reflected beam can be completely described by  $\tan \Psi$ , which represents the amplitude ratio of the complex reflection coefficients  $r_p$  and  $r_s$ , and by the phase shift difference  $\Delta$  between them. Here "p" stands for parallel and "s" for perpendicularly polarized with respect to the incidence plane. The experimental measurement of these quantities is the subject of spectroscopic ellipsometry. A photometric ellipsometer described in detail elsewhere,<sup>17,18</sup> attached to a Bruker IFS66 Fourier transform spectrometer, was used for all the measurements. The ellipsometric parameters  $\tan \Psi$  and  $\Delta$  were calculated from intensity measurements at four polarizers' azimuths while the analyzer was fixed at 45° with respect to the plane of incidence. A second measurement set performed with a retarder (KRS5 totally reflecting prism) inserted behind the sample, which introduces a known phase shift, allows the accurate determination of  $\Delta$  between 0° and 360° and an increased sensitivity for the evaluation of  $\Delta$  near  $\cos \Delta = \pm 1$ . In the standard ellipsometric setup, using a conventional light source (e.g., glowbar), a sample area of  $10 \times 15 \text{ mm}^2$  is investigated, and the resulting ellipso-

**Figure 2.** Spectral simulation of the ellipsometric parameter  $\Delta$  for the untreated LB film. Experimental (thick line) and calculated (thin line) spectra were fitted to evaluate a refractive index  $n_{\infty} = 1.41$  and thickness of 60 nm. One parameter set was used to model the optical constants at three angles of incidence.

metric spectra represent its average signal. When tiny samples or particular spots within the sample area are to be probed, using tight apertures is mandatory. This, however, leads to signal losses. A highly brilliant IR synchrotron source can enable such investigations of small samples with sufficient signal-to-noise ratios and an increase in the lateral resolution.<sup>19</sup>

**(B) Film Deposition and Thermal Treatment.** The multiple layers of the amphiphilic 2,5-diphenyl-1,3,4-oxadiazole were deposited using the routine LB technique. The substance was first dissolved in chloroform (Merck) to afford a  $2 \times 10^{-3} \text{ M}$  stock solution. Approximately 100  $\mu\text{L}$  of solution was spread onto the water subphase deionized by a milli-Q system (Millipore). Nine double layers were consecutively deposited onto a gold surface (200 nm gold evaporated onto glass slides) at 18 °C and a surface pressure of 28 mN/m.

The samples were heated on a hotplate under ambient conditions. Prior to the treatment, the temperature was raised to 130 °C. The sample was exposed to this temperature for 10 min.

## Calculation

Spectral simulations of the ellipsometric parameters  $\tan \Psi$  and  $\Delta$  were carried out to determine the optical constants and thickness. The best-fit calculation procedure, based on a rigorous  $4 \times 4$  matrix formalism,<sup>20,21</sup> was employed for the evaluation of the ellipsometric spectra. The special optical model of a uniaxial anisotropic film on an isotropic substrate in isotropic ambient conditions holds in general for the investigated LB film. Hence, the simulations within optimization routines were simplified by employing the explicit analytical expressions for this optical model derived from the  $4 \times 4$  matrix formalism and given by Azzam and Bashara.<sup>21</sup> The proposed model accounts for the anisotropic properties of the LB film optical constants and therefore is capable of reproducing the IR band amplitudes as a function of the molecular orientation. The vibrational spectrum was modeled by a sequence of harmonic oscillators.

The routines used for calculations were created in the MATLAB environment, and the MATLAB optimization toolbox was used for the curve-fitting procedure.

## Results and Discussion

**(A) Determination of the Film Thickness.** Figure 2 displays the experimental  $\Delta$  spectra and the simulated

(12) Meuse, C. W. *Langmuir* **2000**, *16*, 9483–9487.

(13) Benferhat, R.; Drevillon, B. *Thin Solid Films* **1988**, *156*, 295–305.

(14) Röseler, A.; Dietel, R.; Korte, E. H. *Microchim. Acta (Suppl.)* **1997**, *14*, 657–661.

(15) Reiche, J.; Knochenhauer, G.; Dietel, R.; Freydank, A.; Zetzsche, T.; Geue, T.; Barberka, T. A.; Pietsch, U.; Brehmer, L. *Supramol. Sci.* **1997**, *4*, 455–459.

(16) Tsankov, D.; Hinrichs, K.; Röseler, A.; Korte, E. H. *Phys. Status Solidi A* **2001**, *188*, 1319–1329.

(17) Röseler, A. *Thin Solid Films* **1993**, *234*, 307–313.

(18) Röseler, A.; Korte, E. H. In *Handbook of Vibrational Spectroscopy*; Griffiths, P. R., Chalmers, J., Eds.; Wiley: Chichester, U.K., 2001; Vol. 2, pp 1065–1090.

(19) Peatman, W. B.; Schade, U. *Rev. Sci. Instr.* **2001**, *72*, 1620.

(20) Schubert, M. *Phys. Rev.* **1996**, *B53*, 4265–4277.

(21) Azzam, R. M. A.; Bashara, N. M. *Ellipsometry and Polarized Light*; North-Holland Publishing Co.: Amsterdam, New York, Oxford, 1977; Chapter 4.

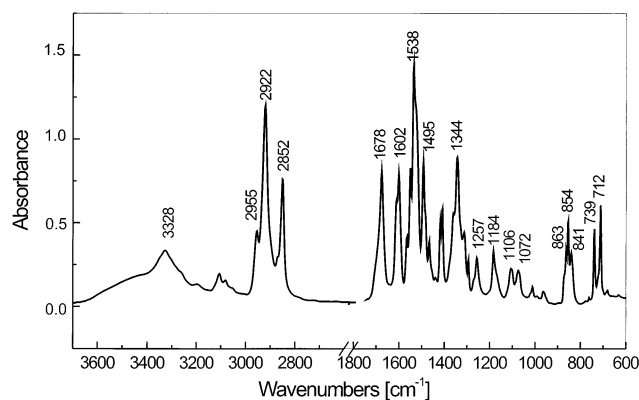


**Figure 3.** IR transmission spectrum of the compound used for preparing the LB film. The spectrum is recorded from a KBr pellet.

spectra by means of best-fit calculations. The initial step in the fitting procedure was the determination of the substrate optical constants. In our case, the optical constants of the gold layer were determined by a separate ellipsometric measurement, although data can also be found in the literature. The fitting procedure for the spectra of the LB film was first applied in a narrow spectral range, where contributions of vibrational features are negligibly small. The procedure yields the high-frequency refractive index  $n_\infty$  and the geometrical thickness  $d$  of the LB film. These data were further optimized to fit the experimental  $\Delta$  spectra taken at three different incidence angles, and the results were refined until the best fit was reached. Following this procedure, improved consistency of the deduced values can be attained. The best fit was found for  $n_\infty = 1.41$  and a thickness of 60 nm for the untreated LB film. It has to be emphasized here that the determined optical constants of films deposited on metals are related to their values in the  $z$ -direction only, where the  $z$ -axis is chosen perpendicular to the substrate surface. The effective electromagnetic field parallel to the metal surface has zero values and therefore does not interact with the film molecules. A 60 nm film thickness for nine double layers seems to exceed the overall molecular length since the extended molecule is about 3 nm. The length abundance could be attributed to the bilayer spacing typical for Y-type LB films.

An identical procedure was also applied to the same LB film after annealing at 130 °C for 10 min. Overall molecular rearrangement was expected to occur as detected by X-ray specular reflectivity (XSR) data.<sup>15</sup> The  $\Delta$  fit evaluation resulted in an average increase of about 5 nm in the thickness of the annealed film. This small increment is slightly greater than the resolvable range given by the error in our evaluations. Therefore, these results could be interpreted only just as a minor indication for an increased film thickness after annealing. One possible explanation could be found in a lowered molecular tilt angle. This assertion, however, needs further verification, which can be made by cautious analysis of the amplitude changes of vibrational peaks as revealed by the ellipsometric spectra. This analysis is given in the section that follows.

**(B) Vibrational Properties.** The IR transmittance spectrum of the 2,5-diphenyl-1,3,4-oxadiazole derivative, recorded in a KBr pellet, is presented in Figure 3. The frequencies of the most prominent IR bands and their tentative assignments are listed in Table 1. For better comparison, the peak wavenumbers of the LB film before and after the thermal treatment, taken from the  $\tan \Psi$  ellipsometric spectra, are also given in the same table, while the  $\tan \Psi$  spectra themselves are displayed in parts

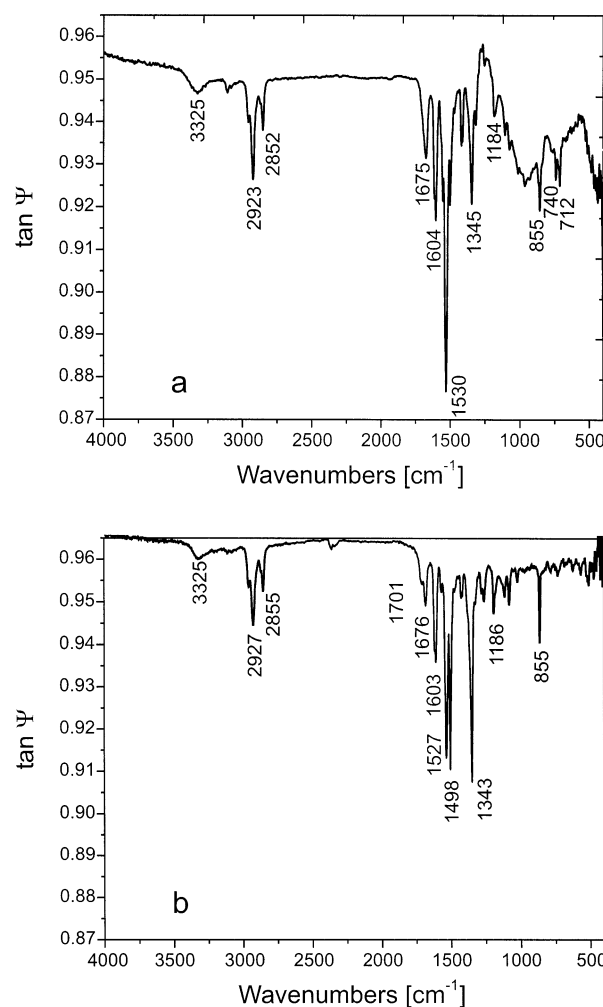


**Figure 4.** Ellipsometric parameter  $\tan \Psi$  of the LB film before (a) and after (b) annealing.

a and b, respectively, of Figure 4. Next to the experimental peak wavenumbers in Table 1, in separate columns, are also presented the vibrational band frequencies as obtained from the best-fit calculations. Fragments of the experimental and the simulated  $\Delta$  and  $\tan \Psi$  spectra of the untreated and the annealed films are displayed in Figure 5. To facilitate the presentation of the qualitative data analysis, we refer to the experimental  $\tan \Psi$  ellipsometric spectra, for which in our case bands of the LB layer on a metal surface have simple "absorption-like" forms. For quantitative considerations, however, the required vibrational band frequencies and oscillator strengths derived from the best-fit calculations of the  $\tan \Psi$  and  $\Delta$  spectra were employed.

The number of bands in the ellipsometric spectra is reduced compared to that of the pellet transmission spectrum. This is a clear indication that some of the bands have negligible transition dipole moments along the surface normal and consequently do not contribute to the spectra according to the so-called surface selection rule.

A brief examination of the spectra shows that the amphiphilic 2,5-diphenyl-1,3,4-oxadiazole molecules are intermolecularly hydrogen bonded both in the pellet and as LB films. The hydrogen bonds are formed between the amide hydrogen atom and the corresponding carbonyl oxygen atom of an adjacent molecule. The band at 3328  $\text{cm}^{-1}$  in the pellet spectrum and the corresponding bands at 3325  $\text{cm}^{-1}$  in the ellipsometric spectra suggest strong hydrogen bonds, which are only partly disrupted after



**Table 1. Most Prominent IR Bands of the LB Molecules and Their Assignments**

$\tilde{\nu}$ (cm <sup>-1</sup> )					
KBr pellet	LB film untreated		LB film annealed		assignment <sup>c</sup>
	exptl <sup>a</sup>	calcd <sup>b</sup>	exptl <sup>a</sup>	calcd <sup>b</sup>	
3328	3325	3323	3325	3326	$\nu$ (NH)
2955	2957	2959	2960	2961	$\nu_{as}$ (CH <sub>3</sub> )
2922	2923	2924	2927	2926	$\nu_{as}$ (CH <sub>2</sub> )
2870	2872	2871	2872	2871	$\nu_s$ (CH <sub>3</sub> )
2852	2852	2852	2855	2853	$\nu_s$ (CH <sub>2</sub> )
			1701	1701	$\nu$ (CO) amide I
1678	1675	1675	1676	1680	$\nu$ (CO) amide I
1612/1602	1614/1604	1614/1602	1612/1603	1613/1601	benzene ring
1538	1530	1527	1527	1525	$\nu_{as}$ (NO <sub>2</sub> )
1495	1500	1496	1498	1496	benzene ring
1344	1345	1346	1343	1341	$\nu_s$ (NO <sub>2</sub> )
1184	1184	d	1186	1184	$\nu$ (C–NO <sub>2</sub> ) str
1106	1106	<i>d</i>	1106	1106	$\delta_{ip}$ (CH) benzene ring
1072	1075	<i>d</i>	1073	1073	
1012	1013	<i>d</i>	1015	1014	$\delta_{ip}$ (CH) benzene ring
963	964	<i>d</i>			oxadiazole ring
863	860	866			$\delta_{oop}$ (CH) benzene ring
854	855	854	855	854	$\delta_s$ (NO <sub>2</sub> )
841	841	838		e	$\delta_{oop}$ (CH) benzene ring
739	740	740			NO <sub>2</sub> wagging
712	712	712		e	

<sup>a</sup> Experimental peak wavenumbers taken from the  $\tan \Psi$  spectra. <sup>b</sup> Calculated band frequencies from the curve-fitting procedure. <sup>c</sup> The band assignments were proved by the reduced IR linear dichroic spectra of the amphiphilic 2,5-diphenyl-1,3,4-oxadiazole compound, dissolved and oriented in a nematic liquid crystal, ZLI 1695 (Merck).<sup>27</sup>  $\delta_{ip}$  = in-plane CH ring deformation mode.  $\delta_{oop}$  = out-of-plane CH ring deformation mode.  $\delta_s$  = symmetric deformation mode. <sup>d</sup> These bands were obscured by a broad SiO<sub>2</sub> band due to the uncovered part of the glass substrate in the experimental spectra, which made impossible their accurate theoretical reproduction.<sup>23</sup> <sup>e</sup> Very weak bands.

the film is annealed at 130 °C. Presumably, they play the role of an additional reinforcement factor, stabilizing the LB structure. The intermolecular hydrogen bonds could also prevent possible crystal packing of the alkyl chains, typically observed for long aliphatic hydrocarbons, as was anticipated in the X-ray study.<sup>15</sup> A characteristic feature of this crystal packing is the band splitting of the CH<sub>2</sub> bending and rocking vibrations that has not been observed in our spectra. This in turn supports the assumption made in the X-ray study.<sup>15</sup>

The ellipsometric spectra of both untreated and annealed samples show all bands due to C–H valence stretching vibrations typical for the long aliphatic hydrocarbons.<sup>22</sup> The presence of all these vibrations implies an overall tilted structure of the aliphatic chains, since both symmetric and antisymmetric transition dipole moments of the methylene groups are mutually orthogonal and at the same time perpendicular to the long molecular axis. Therefore, they would not be excited provided the molecules were standing precisely upright. There was, however, a small but steady overall decrease of the aliphatic CH<sub>2</sub> band amplitudes in the spectra of the annealed film compared to the untreated one (Figure 4). This as well as the overall change by 2–4 cm<sup>-1</sup> of all structurally sensitive band frequencies is an additional clue indicating that a molecular rearrangement had probably occurred due to thermal treatment. The observed 4 cm<sup>-1</sup> frequency upshift in both the  $\nu_s$ (CH<sub>2</sub>) and  $\nu_{as}$ (CH<sub>2</sub>) vibrations could be attributed to an “all-trans–gauche” conformation transition in the annealed LB film, implying an all-trans conformation of the untreated film. The presence of a progressive band structure that is another characteristic feature of the all-trans conformation of the alkyl chains is not clearly detected in the spectrum presented in Figure 4a. This band structure involves a mixture of CH<sub>2</sub> wagging, twisting, and rocking vibrations and emerges in the 1150–1450 cm<sup>-1</sup> region,<sup>22</sup> but this

range is partly obscured by a broad SiO<sub>2</sub> band originating from an uncovered part of the glass substrate.<sup>23</sup> The weakening of the CH<sub>2</sub> band amplitudes could be associated with lowering of the average tilt angle of the LB molecules. This assertion, however, needs further proof.

The aromatic C–H stretching vibrations originating from the two phenyl rings which typically appear above 3000 cm<sup>-1</sup> are significantly less pronounced, according to their lower molar absorptivities. Although the annealed sample also exhibits reduced aromatic band intensities, these bands are rarely used as structural markers due to their commonly weak band amplitudes.

The carbonyl band at 1678 cm<sup>-1</sup> (amide I) is slightly shifted down by 3 cm<sup>-1</sup> in both treated and untreated LB films in comparison to the KBr pellet. The shoulder evident in the untreated film emerges as a separate band located at 1701 cm<sup>-1</sup> for the annealed sample. This band splitting points to partial disruption of the hydrogen bonds after the thermal treatment. Judging by the band amplitudes, the dominant part of the molecules still remains hydrogen bonded. An expected corresponding appearance of a free NH band around 3430 cm<sup>-1</sup>, however, is not detected, likely because the *z*-component (*z*-axis coinciding with the surface normal) of its transition moment is negligibly small.

The most striking differences between the two  $\tan \Psi$  spectra are observed in the region where the NO<sub>2</sub> group absorbs. The two NO<sub>2</sub> stretching vibrations, namely, the symmetric one at 1345 cm<sup>-1</sup> and the antisymmetric one at 1530 cm<sup>-1</sup>, are clearly observed in both spectra. These vibrations in the bulk spectrum exhibit comparable band intensities, while the ellipsometric spectra of the untreated

(22) Snyder, R. G.; Schahtschneider, J. H. *Spectrochim. Acta* **1963**, *19*, 85–116.

(23) Measuring the untreated LB film, we omitted to cover the substrate glass slide outside the sample area, which caused the broad absorption band around 1000 cm<sup>-1</sup>. When the actual reason for that was established, it was too late to repeat the experiment, since the sample was already annealed. This, however, prompted us to carefully cover the substrate surface prior to the measurement of the thermally treated LB film, so any contributions from SiO<sub>2</sub> were avoided in the spectrum in Figure 4b.

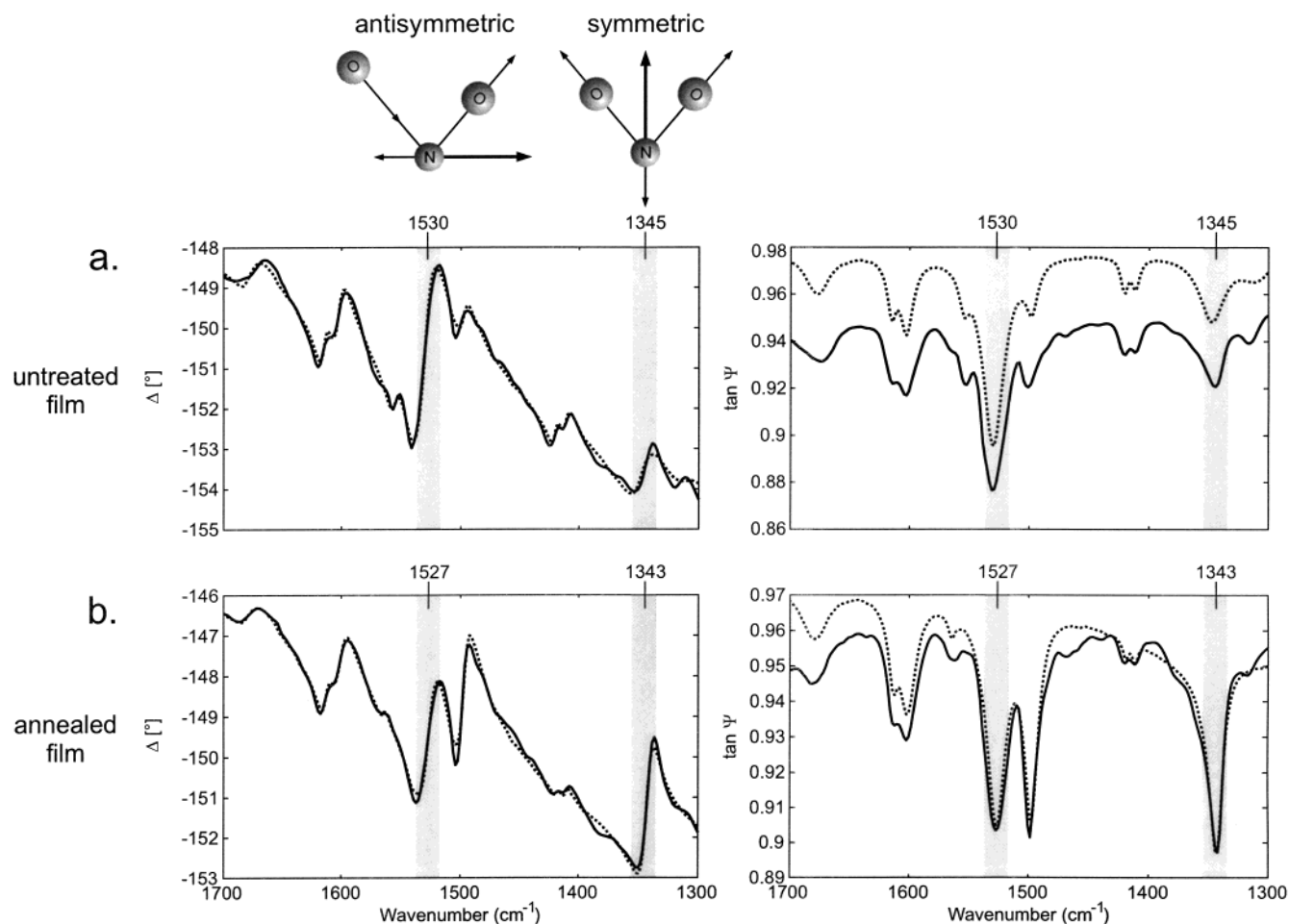


**Figure 5.** Experimental (thick line) and calculated (dashed line) ellipsometric spectra of the LB film before (a) and after (b) annealing. The fragment of the spectra shows the region of the NO<sub>2</sub> stretching bands. The parameters of the oscillator strengths taken from these calculations were used to determine the change of the tilt angle after annealing.

LB film show much stronger bands of the antisymmetric vibration (Figure 4a). Since the transition moments of the two NO<sub>2</sub> vibrations are mutually orthogonal, the significantly enhanced band amplitude of the antisymmetric mode hints to a specific orientation of this group. Such an orientation demands a larger projection of the NO<sub>2</sub> antisymmetric transition moment onto the surface normal than the symmetric one does, as schematically shown in Figure 6. The projection ratio of the symmetric and antisymmetric transition moments onto the z-axis could be deduced from the corresponding band amplitudes after being normalized by the same ratio taken from the bulk spectrum. While this procedure could in principle lead to determination of the angle which the NO<sub>2</sub> groups make to the surface normal,<sup>24</sup> the accurate determination of the overall molecular tilt angle is hampered by the nonlinear shape of the molecule; its 2,5-diphenyl-1,3,4-oxadiazole fragment is bent in the molecular plane and then twisted with respect to the aliphatic tail.

Considerable changes are observed for the same bands when they are compared to those of the annealed sample. The amplitude of the antisymmetric NO<sub>2</sub> band decreases, while the symmetric one is substantially increased and becomes the most prominent band in the spectrum (Figure 4b).

A relative increase of band amplitudes is also observed for the bands at 855, 1186, and 1500 cm<sup>-1</sup>. The first two

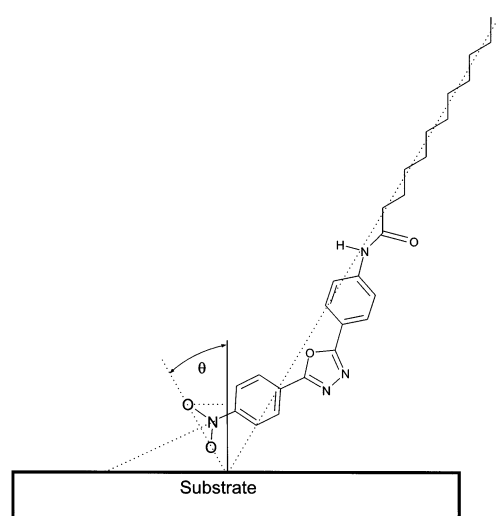


**Figure 6.** Schematic illustration of the molecular orientation of the studied LB film.  $\theta$  is the angle defined by the line connecting the oxygen atoms and the surface normal.

bands represent the NO<sub>2</sub> deformation and C–NO<sub>2</sub> stretching vibrations, respectively. These bands are highly diagnostic since their transition moments are precisely oriented along the molecular long axis, as was demonstrated by the reduced linear dichroic spectra of *p*-nitrobenzaldehyde dissolved and oriented in a nematic liquid crystal matrix.<sup>25</sup> The transition moment of the

(24) Allara, D. L.; Nuzzo, R. G. *Langmuir* **1985**, *1*, 52–66.

phenyl vibration at  $1500\text{ cm}^{-1}$  having the same direction apparently also contributes to its enhanced intensity.

All these arguments point to the occurrence of a macroscopic molecular rearrangement connected with lowering of the tilt angle due to the thermal treatment. Interesting is the behavior of the CH ring out-of-plane bands at  $860$  and  $840\text{ cm}^{-1}$  of the two structurally different phenyl rings, as well as the band due to the  $\text{NO}_2$  wagging vibration at  $740\text{ cm}^{-1}$ . The transition moments of all these vibrations are oriented perpendicularly to the phenyl rings. While well pronounced in the pellet spectrum, the CH ring out-of-plane modes almost vanish in the spectrum of the untreated sample (Figure 4b). This indicates close to parallel orientation of these transition moments with respect to the direction within the substrate plane. The same behavior was also expected for the  $\text{NO}_2$  wagging vibration at  $740\text{ cm}^{-1}$ , which has the same orientation of its transition moment. Its appearance, however, as a weak band in the spectrum of the untreated sample suggests some bent structure of the whole aromatic fragment. This assumption is currently being examined by molecular mechanics calculations. These bands as well as the band located at  $712\text{ cm}^{-1}$  disappear in the spectrum of the annealed sample, signifying complete parallel orientation of their transition moments relative to the substrate surface.

The calculated ellipsometric spectra in the range of the  $\text{NO}_2$  stretching vibrations are presented in Figure 5. The complete good agreement between the experimental and the calculated spectra even in small details strengthens the reliability of the interpretation. If we assume that the molar absorptivities for the symmetric and antisymmetric  $\text{NO}_2$  modes are not essentially different in a pellet and in an LB film, then some quantitative conclusions about the headgroup orientation to the surface normal can be drawn. Judging by the ratio of the parameters of the oscillator strengths for the symmetric and antisymmetric  $\text{NO}_2$  modes, we can estimate the angle  $\theta$  that the line connecting the oxygen atoms makes with the surface normal (Figure 6). The theoretical basis for these calculations was given by Allara and Nuzzo.<sup>24</sup> The calculations showed that the angle  $\theta$  changes from  $39^\circ$  for the untreated film to  $53^\circ$  for the annealed one. A commensurable lowering of the molecular tilt angle is therefore expected although its accurate value cannot be extracted from these data, due to reasons already mentioned in this section. Detailed analysis of the molecular orientation and consistent results

for the tilt angle will be possible when ellipsometric data of the LB films deposited on nonmetallic solids are also available. They will provide data for the transition moments projected parallel to the substrate plane. Another cooperative IR ellipsometric and polarized reflection spectroscopy study on uniaxial polyimide films on silicon substrate was proven successful in the determination of accurate values of the anisotropic optical constants.<sup>28</sup> Such investigations for LB films are currently in progress, they are backed up by molecular mechanics calculations, and the results will be reported later. Then, the more rigorous approach for estimating data for the transition moments parallel to the substrate plane<sup>6,26</sup> will be applied.

### Conclusion

The IR spectroscopic ellipsometry study of Langmuir–Blodgett double layers of 2-[4-(*N*-dodecanoylamino)phenyl]-5-(4-nitrophenyl)-1,3,4-oxadiazole on gold and transmission measurements of a KBr pellet indicate that the molecules are hydrogen bonded both in the pellet and in the LB film. These hydrogen bonds additionally stabilize the LB films and are only partly disrupted after thermal treatment at  $130^\circ\text{C}$ . The ellipsometric results interpreted by best-fit calculations indicate a weak increase of the LB thickness after the sample is annealed. This is explained by a molecular rearrangement and particularly by lowering of the overall molecular tilt angle. Qualitative results derived from best-fit calculations point to a change of about  $14^\circ$  of the angle that the head  $\text{NO}_2$  group makes with the surface normal.

In the present study we demonstrate the potential of IR spectroscopic ellipsometry to analyze both the optical and the structural properties of thin molecular layers and to reveal some aspects of the molecular orientations.

**Acknowledgment.** We are indebted to Prof. B. Jordanov, Institute of Organic Chemistry, Bulgarian Academy of Sciences, for helpful discussions. Thanks are due to Dr. S. Katholy and Dr. B. Schulz, University of Potsdam, Germany, for cooperation and Ms I. Fischer for technical assistance. Financial support by the Deutsche Forschungsgemeinschaft, the Senatsverwaltung für Wissenschaft, Forschung und Kultur des Landes Berlin, and the Bundesministerium für Bildung und Forschung is gratefully acknowledged.

LA0201117

(25) Kerezstury, G.; Jordanov, B.; Sundius, T. *Proceedings of the 12th ICOFTS*, Tokyo; Waseda University Enterprise Press: Tokyo, 1999; pp 531–532.

(26) Hasegawa, T.; Takeda, S.; Kawaguchi, A.; Umemura, J. *Langmuir* **1995**, *11*, 1236–1243.

(27) Jordanov, B.; Tsankov, D.; Hinrichs, K.; Dietel, R.; Korte, E. H. To be published.

(28) Hinrichs, K.; Tsankov, D.; Korte, E. H.; Röseler, A.; Sahre, K.; Eichhorn, K.-J. *Appl. Spectrosc.*, in press.